Report from the LBNE Reconfiguration Physics Working Group

J. Appel, M. Bishai, S. Brice, E. Blucher, M. Diwan, B. Fleming, G. Gilchriese, W. Marciano, M. Messier, S. Parke, J. Reichanadter, G. Rameika, K. Scholberg, M. Shochet†, J. Thomas, C. Young, G. Zeller,

†*Physics Working Group Chair*

(Dated: May 6, 2012)

This report has been prepared by the LBNE Reconfiguration Physics Working Group at the request of the LBNE Reconfiguration Steering Committee.

CONTENTS

I. Introduction 1

II. Configurations 1

III. Long-Baseline Physics 2
- A. The Neutrino Beams 4
- B. The LAr-TPC Neutrino Detector 5
- C. Mass Hierarchy and CP Violation Sensitivity 6
- D. Precision Measurement of Neutrino Mixing Parameters 13
- E. Searches for New Physics 13
  - 1. Non-standard Interactions 13
  - 2. Long-Range Interactions 13
  - 3. Search for Active-Sterile Neutrino Mixing 13
- F. Summary 14

IV. Non-Accelerator Physics Reach 16

V. Summary 19

References 20

I. INTRODUCTION

This report has been prepared by the LBNE Reconfiguration Physics Working Group at the request of the LBNE Reconfiguration Steering Committee.

II. CONFIGURATIONS

Config. Number	Beam	Baseline	Location	Depth	Detector
1	NuMI LE	735km	Soudan	0	LAr 5, 10, 15, 34 kt
2	NuMI LE	735km	Soudan	2300ft	LAr 5, 10, 15, 34 kt
3	NuMI ME	810km	Ash River	0	LAr 5, 10, 15, 34 kt
4	NuMI ME	810km	Ash River	0	TASD 14 (NOνA), 40kt
5	NuMI LE	1000km	Canada	0	LAr 5, 10, 15, 34 kt
6	LBNE LE	1300km	Homestake	0	LAr 5, 10, 15, 34 kt
7	LBNE LE	1300km	Homestake	4850ft	LAr 5, 10, 15, 34 kt
8	LBNE pME	2500km	West Coast	??	LAr 5, 10, 15, 34 kt

TABLE I. Summary of the configurations considered by the LBNE Reconfiguration Physics Working Group.

III. LONG-BASELINE PHYSICS

Although the Standard Model of particle physics presents a remarkably accurate description of the elementary particles and their interactions, it is known that the current model is incomplete and that a more fundamental underlying theory must exist. Results from the last decade, that the three known types of neutrinos have nonzero mass, mix with one another and oscillate between generations, implies physics beyond the Standard Model [?].

The three-flavor-mixing scenario for neutrinos can be described by three mixing angles (θ_{12}, θ_{23} and θ_{13}) and one CP-violating phase (δ_{CP}). The probability for neutrino oscillation also depends on the difference in the squares of the neutrino masses, $\Delta m^2_{ij} = m^2_i - m^2_j$; three neutrinos implies two independent mass-squared differences (Δm^2_{21} and Δm^2_{32}).

The entire complement of neutrino experiments to date has measured five of the mixing parameters: three angles, θ_{12}, θ_{23}, and recently θ_{13}, and two mass differences, Δm^2_{21} and Δm^2_{32}. The sign of Δm^2_{21} is known, but not that of Δm^2_{32}. The value of θ_{13} has been determined to be much smaller than the other two mixing angles [?] [?], implying that mixing is quantitatively different in the neutrino and quark sectors. Table II summarizes the current values of the neutrino oscillation parameters obtained from a global fit to experimental data [?] and the measurement of θ_{13} from the Daya Bay reactor experiment [?]. A comparison to the equivalent mixing parameter values in the CKM matrix are also shown.

TABLE II. Best fit values of the neutrino mixing parameters in the PMNS matrix and comparison to the equivalent values in the CKM matrix

Parameter	Value (PMNS)	Value (CKM)
θ_{12}	$34 \pm 1^\circ$	$13.04 \pm 0.05^\circ$
θ_{23}	$43 \pm 4^\circ$	$2.38 \pm 0.06^\circ$
θ_{13}	$9 \pm 1^\circ$	$0.201 \pm 0.011^\circ$
Δm^2_{21}	$+(7.58 \pm 0.22) \times 10^{-5}$ eV^2	
Δm^2_{32}	$\lvert(2.35 \pm 0.12)\rvert \times 10^{-3}$ eV^2	$m_3 >> m_2$
δ_{CP}	no measurement	$67 \pm 5^\circ$

Assuming a constant matter density, the oscillation of $\nu_\mu \to \nu_e$ in the Earth for 3-generation mixing is described approximately by the following equation [?]

$$\begin{aligned} P(\nu_\mu \to \nu_e) \approx \sin^2\theta_{23} &\frac{\sin^2 2\theta_{13}}{(\hat{A}-1)^2}\sin^2((\hat{A}-1)\Delta) \\ &+\alpha\frac{\sin\delta_{CP}\cos\theta_{13}\sin 2\theta_{12}\sin 2\theta_{13}\sin 2\theta_{23}}{\hat{A}(1-\hat{A})}\sin(\Delta)\sin(\hat{A}\Delta)\sin((1-\hat{A})\Delta) \\ &+\alpha\frac{\cos\delta_{CP}\cos\theta_{13}\sin 2\theta_{12}\sin 2\theta_{13}\sin 2\theta_{23}}{\hat{A}(1-\hat{A})}\cos(\Delta)\sin(\hat{A}\Delta)\sin((1-\hat{A})\Delta) \\ &+\alpha^2\frac{\cos^2\theta_{23}\sin^2 2\theta_{12}}{\hat{A}^2}\sin^2(\hat{A}\Delta) \end{aligned} \tag{1}$$

where $\alpha = \Delta m^2_{21}/\Delta m^2_{31}$, $\Delta = \Delta m^2_{31}L/4E$, $\hat{A} = 2VE/\Delta m^2_{31}$, $V = \sqrt{2}G_F n_e$. n_e is the density of electrons in the Earth. Recall that $\Delta m^2_{31} = \Delta m^2_{32} + \Delta m^2_{21}$. Also notice that $\hat{A}\Delta = LG_F n_e/\sqrt{2}$ is sensitive to the sign of Δm^2_{31}. For antineutrinos, the second term in Equation 1 has the opposite sign, and the matter potential also has the opposite sign. The second term is proportional to the following CP violating quantity:

$$J_{CP} \equiv \sin\theta_{12}\sin\theta_{23}\sin\theta_{13}\cos\theta_{12}\cos\theta_{23}\cos^2\theta_{13}\sin\delta_{CP} \tag{2}$$

Equation 1 is an expansion in powers of α. The $\nu_\mu/\bar{\nu}_\mu \to \nu_e/\bar{\nu}_e$ oscillation probabilities from the approximate forumla given in Equation 1 as a function of neutrino energy and baseline are shown in Figure 1 for both the normal mass hierarchy ($m_1 < m_2 < m_3$) and inverted mass hierarchy ($m_3 < m_1 < m_2$) . There are two very different oscillation scales driven by the two independent mass-squared differences (Δm^2_{21} and Δm^2_{32}). The maximal oscillation

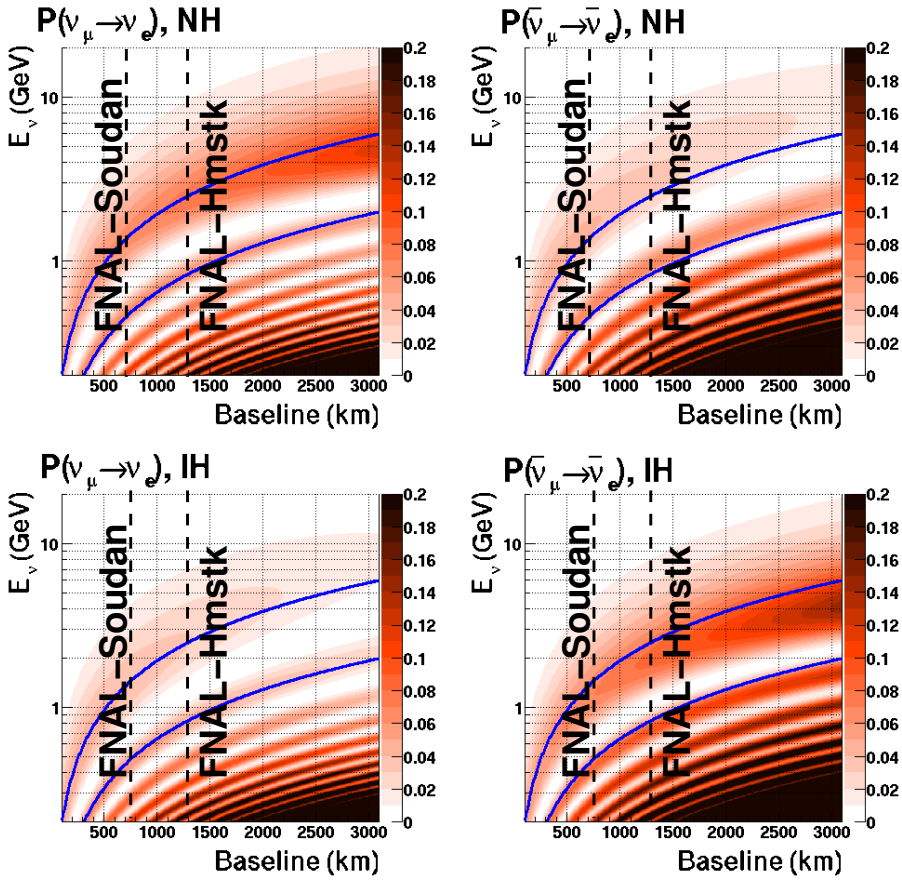

FIG. 1. The $\nu_\mu/\bar{\nu}_\mu \to \nu_e/\bar{\nu}_e$ oscillation probability vs neutrino energy and baseline with $\sin^2 2\theta_{13} = 0.1, \delta_{cp} = 0$ for normal hierarchy (top) and inverted hierarchy (bottom). The solid blue lines correspond to the locations of the 1st and 2nd oscillation maxima in vacuum.

probabilities occur at:

$$\begin{aligned} L/E_\nu^n \text{ (km/GeV)} &= (2n-1)\frac{\pi}{2}\frac{1}{(1.267 \times \Delta m^2 \text{ (eV}^2))} \\ &\approx (2n-1) \times 500 \text{ km/GeV for } \Delta m^2_{32} \text{ (atmospheric)} \\ &\approx (2n-1) \times 15,000 \text{ km/GeV for } \Delta m^2_{21} \text{ (solar)} \end{aligned} \tag{3}$$

where E_ν^n is the neutrino energy at the maxima of oscillation node n. The oscillations of $\nu_\mu \to \nu_e$ in long baseline accelerator neutrino experiments are driven primarily by the atmospheric mass scale. The 1st and 2nd nodes are indicated as solid blue lines in Figure 1. The approximate formula given in Equation 1 is useful for understanding important features of the appearance probability shown in Figure 1:

1. The first three terms in the equation control the matter induced enhancement for normal mass ordering ($m_1 < m_2 < m_3$) or suppression for the inverted mass ordering ($m_3 < m_1 < m_2$) which dominates in the region of the first oscillation node (largest E_ν).

2. The second and third terms control the sensitivity to CP and the value of δ_{cp} at the second oscillation node.

3. The last term controls the sensitivity to Δm^2_{21} and the solar oscillation parameters at the higher order oscillation nodes (largest L/E).

4. The first term (last term) is also proportional $\sin^2\theta_{23}$ ($\cos^2\theta_{23}$), and therefore is sensitive to the issue of maximum mixing in $\theta_{23} = \pi/4$.

The large non-zero value of θ_{13} indicates that measurement of the spectrum of oscillated $\nu_\mu \to \nu_e$ events over a large range of L/E in a single experiment will allow us access to all of the parameters in Equation 1 with good systematics control. Figure 1 demonstrates that the longer the experimental baseline the more oscillation nodes and the larger the range of L/E values accessible.

The signature of CP violation is a difference in the probabilities for $\nu_\mu \to \nu_e$ and $\overline{\nu}_\mu \to \overline{\nu}_e$ transitions. The CP asymmetry $\mathcal{A}_{cp}$ is defined as

$$\mathcal{A}_{cp}(E_\nu) = \left[\frac{\mathrm{P}(\nu_\mu \to \nu_e) - \bar{\mathrm{P}}(\bar{\nu}_\mu \to \bar{\nu}_e)}{\mathrm{P}(\nu_\mu \to \nu_e) + \bar{\mathrm{P}}(\bar{\nu}_\mu \to \bar{\nu}_e)}\right] \tag{4}$$

The observed asymmetry $\mathcal{A}$ is a combination of both the CP asymmetry and the asymmetry due to the matter effect. Figure 2 shows the maximal possible CP asymmetry in vacuum ($\delta_{cp} = -\pi/2$) and the asymmetry from the matter effect alone as a function of energy and baseline. The CP asymmetry arising from non-zero/π values of δ_{cp} is dominant in the L/E regions of the secondary oscillation nodes and is independent of baseline, whereas the asymmetry due to the matter effect dominates the region of the first oscillation node and increases with longer baselines.

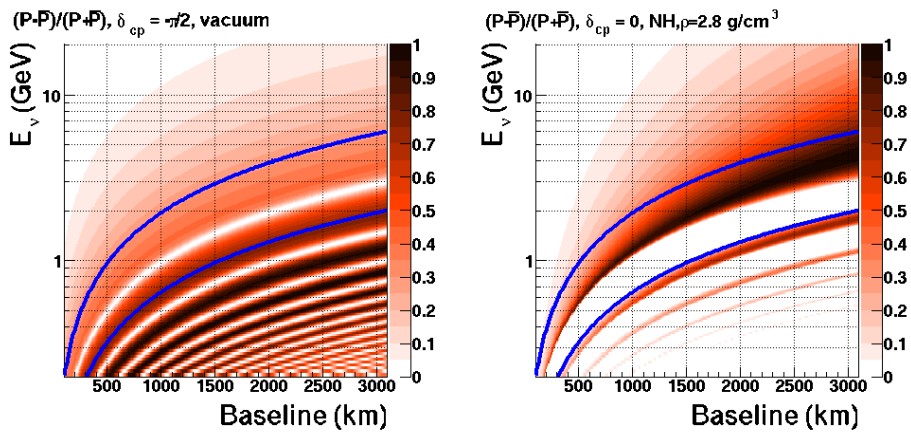

FIG. 2. The asymmetry, $\mathcal{A}_{cp}$, for maximal CP violation in vacuum (left) and arising from the matter effect only (right) as a function of energy and baseline. An average earth density of $\rho = 2.8$ g/cm^3 is assumed for the matter effect.

Observations of $\nu_\mu \to \nu_e$ oscillations of a beam (composed initially of muon neutrinos, ν_μ) over a long baseline and a wide range of neutrino energies are thus the key to unambiguously determining the mass hierarchy (the sign of Δm^2_{32}), and the unknown CP-violating phase δ_{cp}. The study of $\nu_\mu \to \nu_e$ oscillations can also help determine the θ_{23} quadrant since the second and third terms in Equation 1 are proportional to $\sin 2\theta_{23}$.

The study of the disappearance of ν_μ probes $\sin^2 2\theta_{23}$ and —Δm^2_{32}—. The Non-standard physics can manifest itself in differences observed in higher precision measurements of ν_μ and $\bar{\nu}_\mu$ disappearance over long baselines and in observing deviations from the 3-flavor model in $\nu_\mu \to \nu_e$ oscillations. The precision with which we know the current set of neutrino oscillation parameters ensures that the compelling physics program outlined is feasible with the combination of a long baseline, very large detector mass, and a wide-band beam with beam energies matched to the baseline as summarized in Equation 3.

A. The Neutrino Beams

The three beam configurations under consideration are the 1) LBNE beam-line in the low energy configuration on-axis with a detector at Homestake Mine (1300km), 2) the NuMI beam-line in the low energy configuration with a detector on-axis at Soudan Mine (735km), and 3) the NuMI beam-line in the medium energy configuration with a detector 14mrad off-axis at Ash River (810km). The neutrino beam-line parameters used in the GEANT3 simulation for each of these options are summarized in Table III.

All the beam-line designs considered can be operated in neutrino or anti-neutrino mode by reversing the horn current to charge select positive or negative hadrons. The ν_μ and $\bar{\nu}_\mu$ charged current spectra at each candidate far detector location are shown in Figure 3 with the ν_e probability appearance curves overlaid. We note that there is a small beam ν_e contaminant of order 1% from μ and Ke3 decays. There is also a wrong-sign ν_μ contaminant in each beam ($\approx 10\%$) from decays of unfocused hadrons.

TABLE III. The NuMI and LBNE neutrino beam configurations used in this study

	LBNE LE [a]	NuMI LE	NuMI ME
Primary beam	120 GeV p^+	120 GeV p^+	120 GeV p^+
Beam power	708 kW	708 kW	708 kW
POT/yr	6.0×10^{20}	6.0×10^{20}	6.0×10^{20}
Target material	graphite	graphite	graphite
Target cross-section	circular d=1.2cm	rectangular w=0.64cm h=2cm	rectangular w=0.64cm h=2cm
Target length	2 interaction lengths	2 interaction lengths	2 interaction lengths
Focusing horns (1/2)	NuMI, 250kA	NuMI, 185 kA	NuMI, 200 kA
Horn separation	6m	10m	23m
Target-Horn 1 distance	30cm	45cm	135 cm
Decay pipe	4m diameter, 280m long	2m diameter, 677m long	2m diameter, 677m long
	Evacuated/He filled	He filled	He filled

[a] The LBNE decay pipe in the conceptual design has a length between 200 and 250m and is filled with air

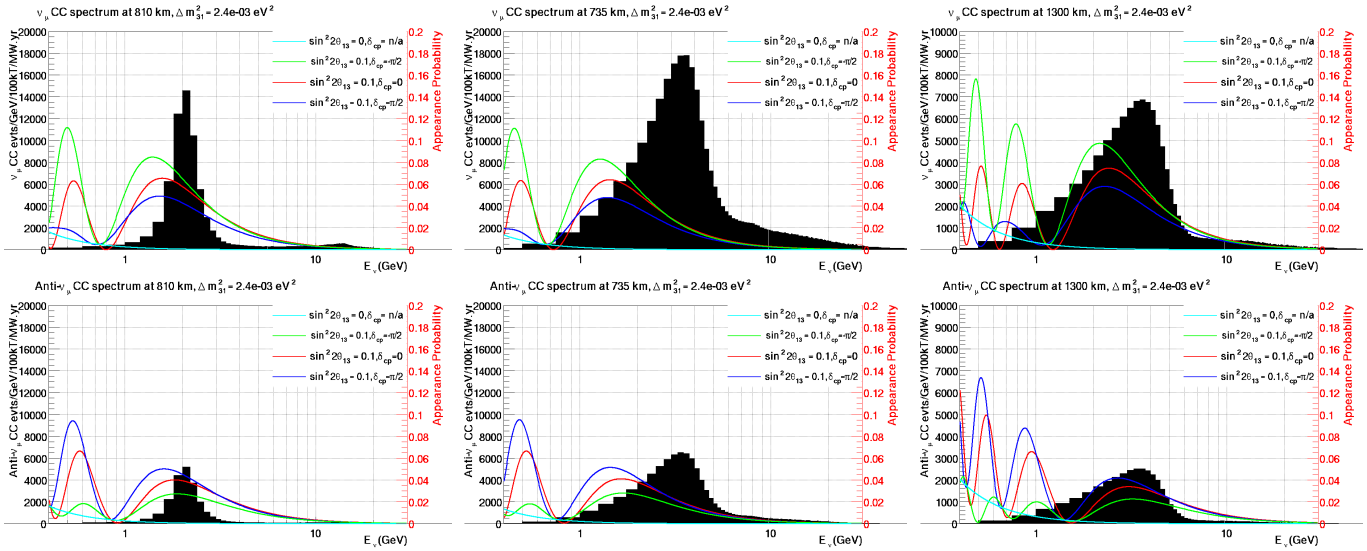

FIG. 3. The Fermilab unoscillated ν_μ CC spectra at the 3 candidate locations (black histograms) with the ν_e appearance probability curves for $\sin^2 2\theta_{13} = 0.1, \delta_{cp} = 0$ (red) $\pi/2$ (blue) $-\pi/2$ (green) with normal mass ordering. The curve in cyan shows the contribution from the fourth term of Equation 1 which is driven by the solar oscillation and is independent of $\sin^2 2\theta_{13}$ and δ_{cp}. The figures are from left to right: NuMI ME at Ash River, NuMI LE at Soudan and the LBNE beam at Homestake. The top set of figures is for neutrino running and the bottom set of figures is for anti-neutrino running

B. The LAr-TPC Neutrino Detector

Neutrino events detected in experiments like LBNE are often categorized according the particle mediating the interaction. The term (used below, and throughout this document) "neutral current process" (NC) refers to an interaction which is mediated by the neutral boson Z^0. Similarly, a "charged current" (CC) interaction involves a postive or negative charged W boson. The flavor of a neutrino in a CC interaction is tagged by the flavor of the emitted lepton: e, μ, τ tag ν_e, ν_μ, ν_τ interactions. A "quasi-elastic" (QE) event is a CC event in which the scattering of the neutrino is almost elastic with only a charged lepton and a nucleon or nucleons emerging from the target nucleus.

TABLE IV. CC interaction rates per 100kT.MW.yrs (1 MW.yr= 1×10^{21} protons-on-target) for $\sin^2 2\theta_{13} = 0.1, \delta_{cp} = 0$, normal mass ordering in the energy range 0.5 to 20 GeV

Expt	ν_μ CC	ν_μ CC osc	ν_μ NC	ν_e beam	$\nu_\mu \to \nu_e$	$\nu_\mu \to \nu_\tau$	$\bar{\nu}_\mu$ CC	$\bar{\nu}_\mu$ CC osc	$\bar{\nu}_\mu$ NC	$\bar{\nu}_e$ beam	$\bar{\nu}_\mu \to \bar{\nu}_e$	$\bar{\nu}_\mu \to \bar{\nu}_\tau$
Ash River 810km	18K	7.3K	360	330	710	38	5.5K	2.0K	305	120	170	
Soudan 735km	73K	49K	1.3K	820	1500	166	27K	18K	1.1K	285	495	54
Hmstk 1300km	29K	11K	500	280	1300	130	11K	3.8K	456	86	273	46

The charged lepton in QE events carries most of the energy of the neutrino, and as a result, QE interactions have the best neutrino-energy resolution. Final State Interactions (FSI) inside the nucleus will alter the expected nucleon types and spectrum, and measurement of this effect is an important goal of the Near Detector. CC and NC interactions of neutrinos with energies > 1 GeV are inelastic and the target nucleus disintegrates producing multiple hadrons.

The cross-section of $\nu/\bar{\nu}$ CC and NC interactions [1] for different event categories is shown in Figure 4.

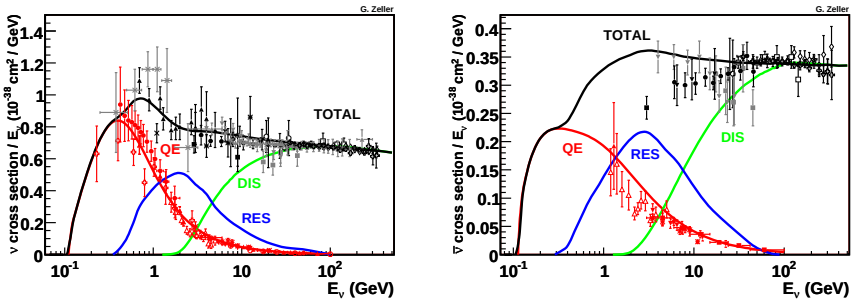

lblfig/nc_xsec.png

FIG. 4. Neutrino charged-current interaction cross-sections for neutrinos (left), and anti-neutrinos (center). The right plot is the NC single π^0 cross-section.

A substantial component of the background for ν_e CC interactions comes from NC interactions where a π^0 is produced. The π^0 decays to two γs which shower electromagnetically and fake electrons. NC interactions where a charged pion is produced are also the predominant background for ν_μ CC interactions where the pion fakes a muon. Therefore to study neutrino flavor oscillations with high precision, the LBNE Far Detector has to have high efficiency, high purity $e/\mu/\gamma$ and $\pi/K/p$ separation.

A massive liquid argon TPC (LArTPC) has been chosen as the Far Detector technology for the LBNE project. TPCs are the detectors of choice for low-rate, large-volume, high-precision particle physics experiments due to their excellent 3D position resolutions and particle identification in large volumes. In addition to detailed event topologies and measurements of particle kinematics, dE/dx measurements allow TPCs to unambiguously distinguish electrons, muons, photons, kaons, pions and protons over a wide range of energies. Examples of how event topologies can be used to identify ν_e/ν_μ CC and ν NC events in a LAr-TPC are shown in Figure 5. The expected signal efficiencies and background mis-identification rates as well as energy resolutions for different event types are summarized in Table V. The performance parameters were derived from several visual scan studies carried out using GEANT4 simulation of LAr-TPC as shown in Figure 5, from studies of the ICARUS detector performance [7–9] and from automated reconstruction used in the 2km LAr detector proposal for the T2K experiment [4].

C. Mass Hierarchy and CP Violation Sensitivity

We use the GLoBeS software package to estimate the significance, σ, with which we can 1) exclude the opposite mass hierarchy, and 2) exclude $\delta_{cp} = 0$ or π (CP violation). A True appearance event spectrum is generated for a given value of $\delta_{cp}, sign(\Delta m^2_{31})$ as shown in Figure 6. A minimum χ^2 fit is performed to the given hypothesis . The minimization accounts for the correlations between the different mixing parameters which are included with Gaussian constraints based on the best fit uncertainties as summarized in Table II. The normalization uncertainties on the signal and background listed in Table V are included as nuisance parameters. θ_{13} is constrained using the projected accuracy expected from the final run of the current reactor experiments (3%). When estimating the sensitivity to the mass hierarchy, the χ^2 minimization is performed over all values of δ_{cp}. The opposite mass hierarchy is included in the minimization when estimating the $\Delta\chi^2$ to determine whether CP is violated ($\delta_{cp} \neq 0$ or π). The significance with which we can exclude the opposite mass hierarchy and determine whether $\delta_{cp} \neq 0$ or π as a function of δ_{cp} is shown in Figure 8 for 3 different LAr-TPC masses, 5, 10, and 34 kT placed at Soudan, Ash River, and LBNE-Homstake. No constraints from other experiments are included.

The significance with which the mass ordering (green) and CP violation is resolved with a LAr-TPC at Ash River and Soudan when combined with NOνA running with the ME beam for 3+3 years (I) and the LE beam for 5+5

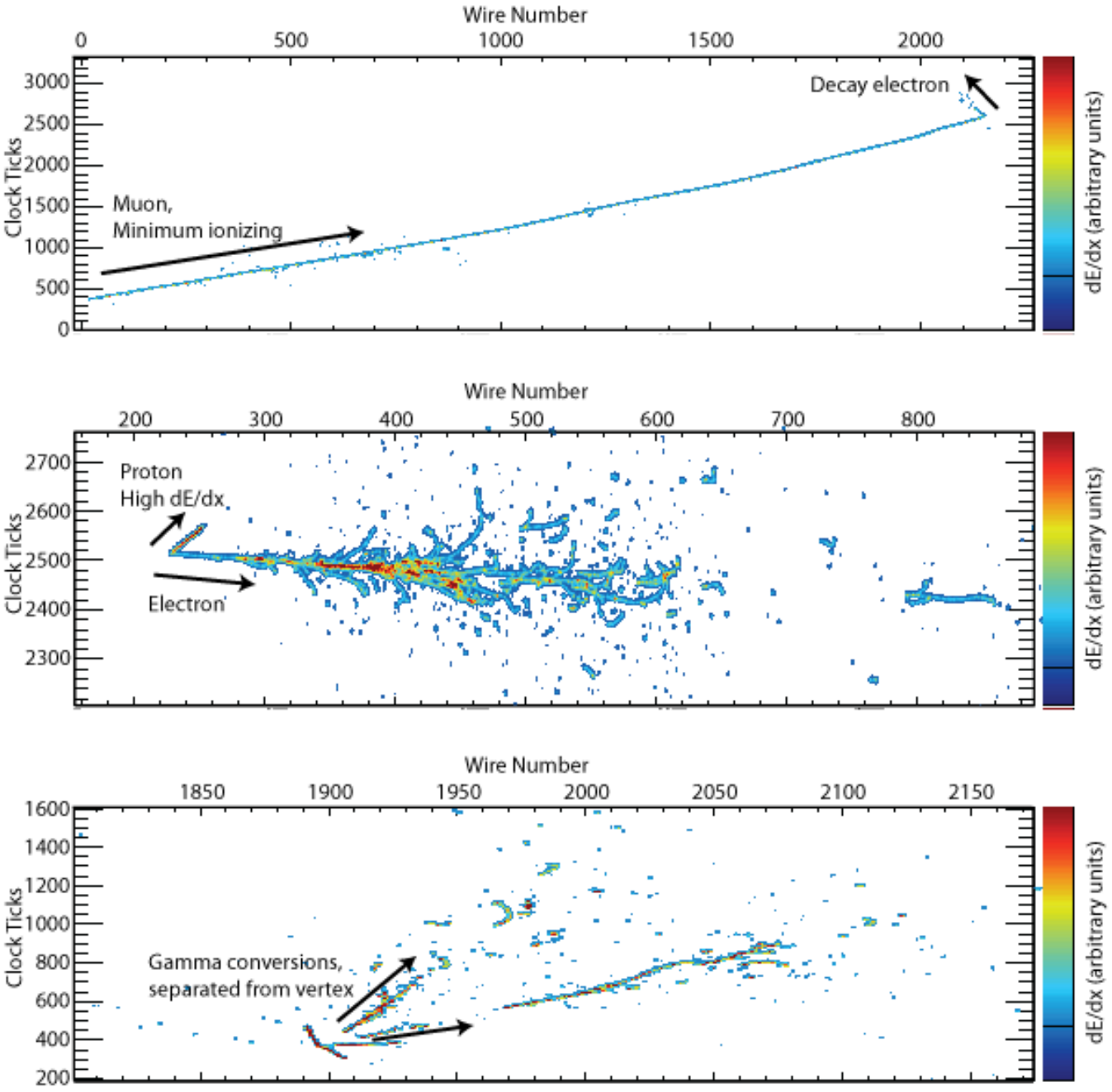

FIG. 5. Examples of neutrino beam interactions in an LArTPC obtained from a GEANT4 simulation [15]. A CC ν_μ interaction with a stopped μ followed by a decay Michel electron (top), a QE ν_e interaction with a single electron and a proton (middle), an NC interaction which produced a π^0 that then decayed into two γ's with separate conversion vertices (bottom)

yrs (II) is shown in Figure 9. The CP violation sensitivity assumes the mass hierarchy will be resolved from the combination of NuMI, NOνA I+II, and T2K [**?**].

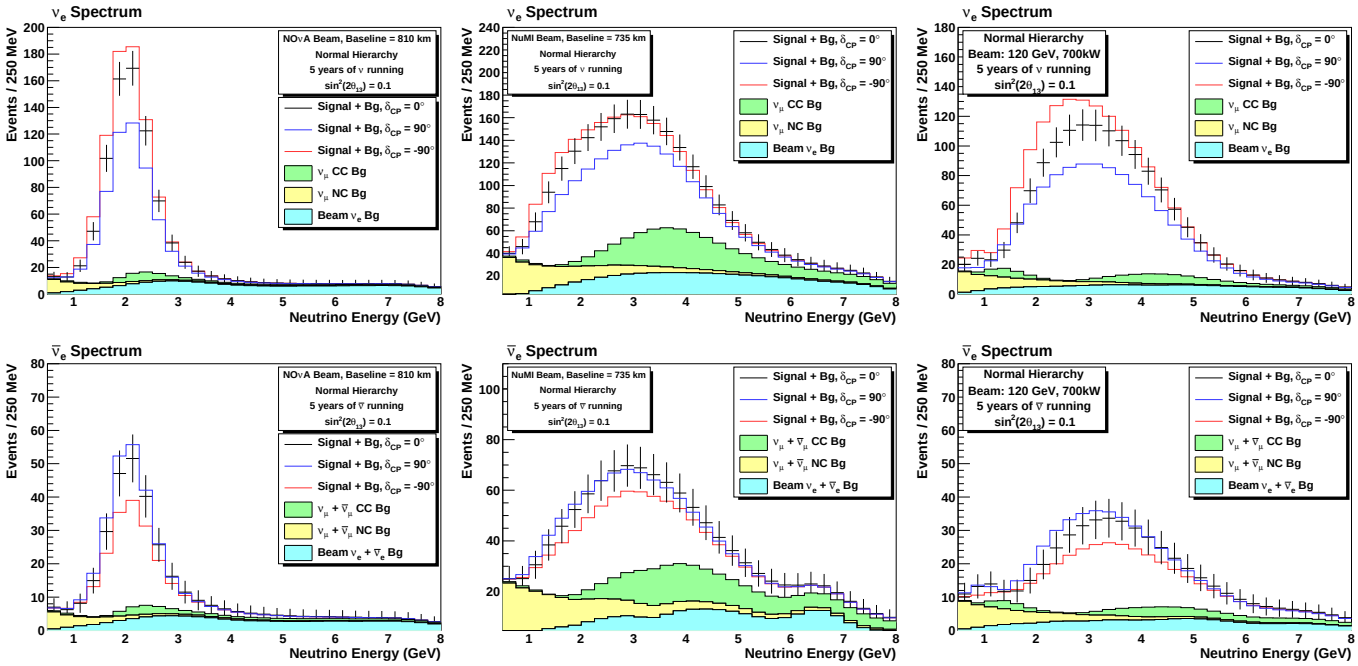

FIG. 6. The expected spectrum of ν_e or $\overline{\nu}_e$ oscillation events in a 34-kton LArTPC for 5 years of neutrino (top) and anti-neutrino (bottom) running with a 700 kW beam assuming $\sin^2(2\theta_{13}) = 0.1$ and normal mass ordering. Backgrounds from intrinsic beam ν_e (cyan), ν_μ NC (yellow), and ν_μ CC (green) are displayed as stacked histograms. The points with error bars are the expected total event rate for $\delta_{cp} = 0$, the red (blue) histogram is the total expected event rate with $\delta_{cp} = -\pi/2(+\pi/2)$. The figures are from left to right: NuMI ME at Ash River, NuMI LE at Soudan and the LBNE beam at Homestake.

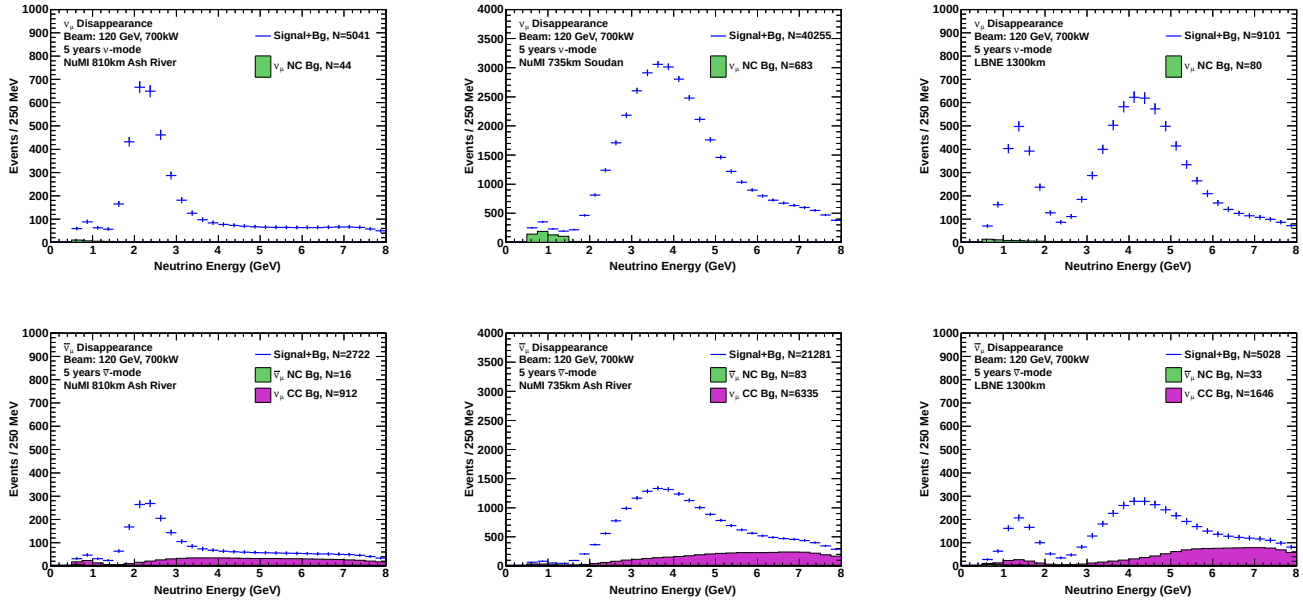

FIG. 7. The expected spectrum of ν_μ or $\overline{\nu}_\mu$ oscillation events in a 34-kton LArTPC for 5 years of neutrino (top) and anti-neutrino (bottom) running with a 700 kW beam. The points with error bars are the expected total event rate for $\Delta^2 m_{32} = 2.35$ and $\sin^2 2\theta_{23} = 0.1$. Backgrounds from NC and the wrong sign ν are displayed. The figures are from left to right: NuMI ME at Ash River, NuMI LE at Soudan and the LBNE beam at Homestake.

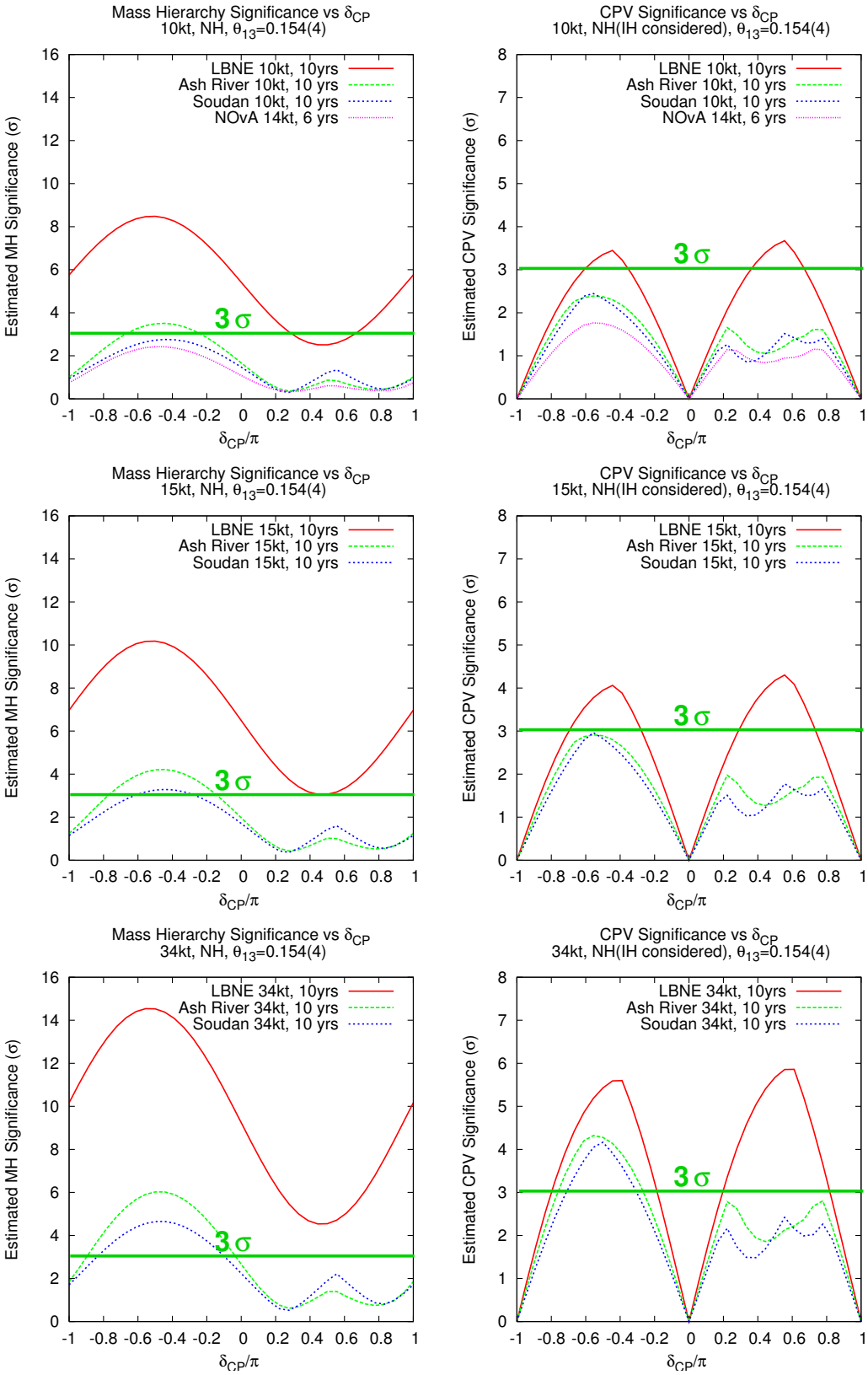

FIG. 8. The significance with which the mass ordering (left) and CP violation ($\delta_{cp} \neq 0, \pi$) is resolved (right) with a LAr-TPC at Ash River (dashed green), Soudan (dashed blue) and LBNE-Homestake (solid red) as a function of the unknown CP violating phase δ_{cp}. The plots are from top to bottom: 10kt, 15kt and 34kt. The significance is calculated using the current constraints on the mixing parameters from the global fit as shown in Table II. θ_{13} is constrained using the projected accuracy expected from the current reactor experiments (3%). The opposite mass hierarchy is considered when calculating the CP violation significance. There is no T2K constraint on the mass hierarchy. An exposure of 5 yrs neutrino running combined with 5 yrs of anti-neutrino running in a 700kW beam is assumed.

TABLE V. Estimated range of the LAr-TPC detector performance parameters for the primary oscillation physics. The expected range of signal efficiencies, background levels, and resolutions from various studies (middle column) and the value chosen for the baseline LBNE neutrino-oscillation sensitivity calculations (right column) are shown. * For atmospheric neutrinos this is the mis-identification rate for < 2 GeV events, the mis-identification rate is taken to be 0 for > 2 GeV.

Parameter	**Range of Values**	**Value Used for LBNE Sensitivities**
Identification of ν_e CC events		
ν_e CC efficiency	70-95%	80%
ν_μ NC mis-identification rate	0.4-2.0%	1%
ν_μ CC mis-identification rate	0.5-2.0%	1%
Other background	0%	0%
Signal normalization error	1-5%	1%
Background normalization error	2-10%	5%
Identification of ν_μ CC events		
ν_μ CC efficiency	80-95%	85%
ν_μ NC mis-identification rate	0.5-10%	0.5%
Other background	0%	0%
Signal normalization error	1-5%	5%
Background normalization error	2-10%	10%
Identification of ν NC events		
ν NC efficiency	70-95%	90%
ν_μ CC mis-identification rate	2-10%	10% *
ν_e CC mis-identification rate	1-10%	10% *
Other background	0%	0%
Signal normalization error	1-5%	
Background normalization error	2-10%	
Neutrino energy resolutions		
ν_e CC energy resolution	$15\%/\sqrt{E(GeV)}$	$15\%/\sqrt{E(GeV)}$
ν_μ CC energy resolution	$20\%/\sqrt{E(GeV)}$	$20\%/\sqrt{E(GeV)}$
E_{ν_e} scale uncertainty		
E_{ν_μ} scale uncertainty	1-5%	2%

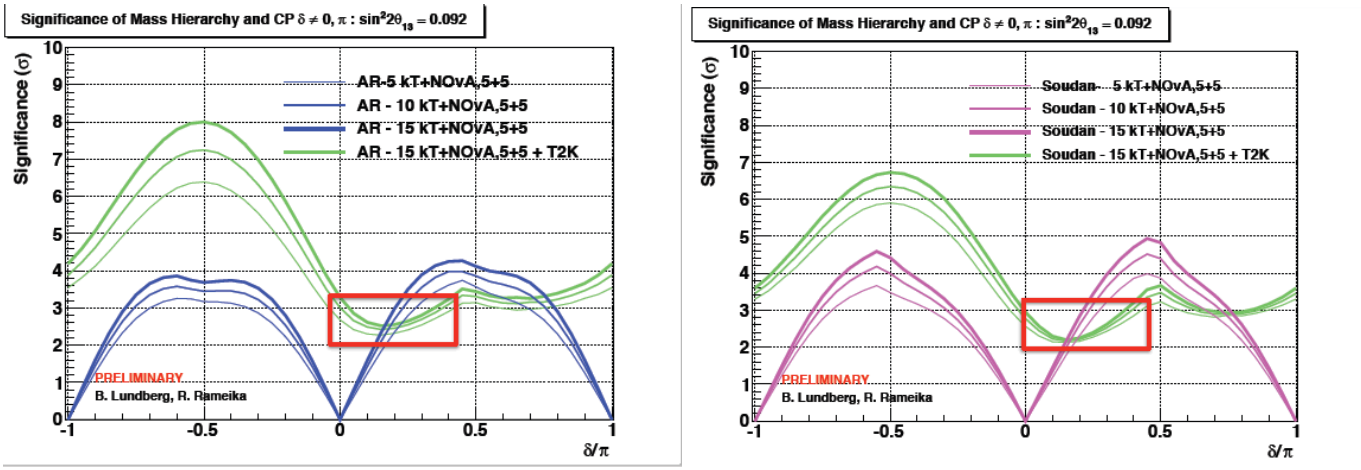

FIG. 9. The significance with which the mass ordering (green) and CP violation is resolved with a LAr-TPC at Ash River (left) and Soudan (right) when combined with NOνA running with the ME beam for 3+3 years (I) and the LE beam for 5+5 yrs (II). The sensitivity to the mass hierarchy also includes the expected constraint from T2K after 7yrs of running at 300kW. The CP violation sensitivity assumes the mass hierarchy will be resolved from the combination of NuMI, NOνA I+II, and T2K. The lines with increasing thickness indicate increasing detector sizes of 5, 10, and 15 kT.

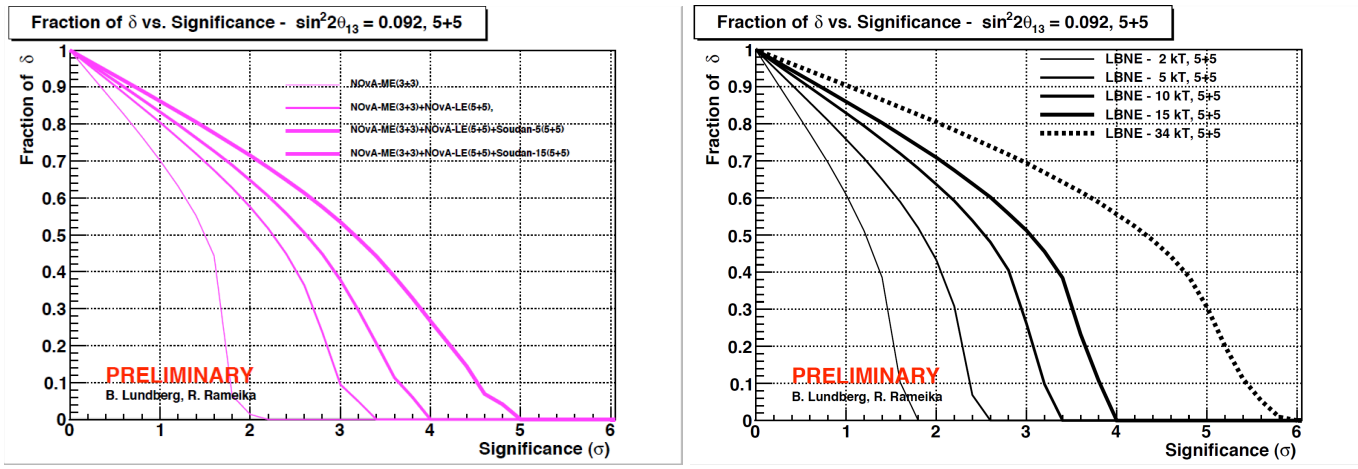

FIG. 10. The fraction of δ_{cp} values for which CP violation is resolved at a given significance. The plot on the left outlines the evolution of the NuMI program when a new LAr-TPC at Soudan is added to extended NOνA running and the plot on the right outlines the reach of LBNE with increasing LAr-TPC detector mass.

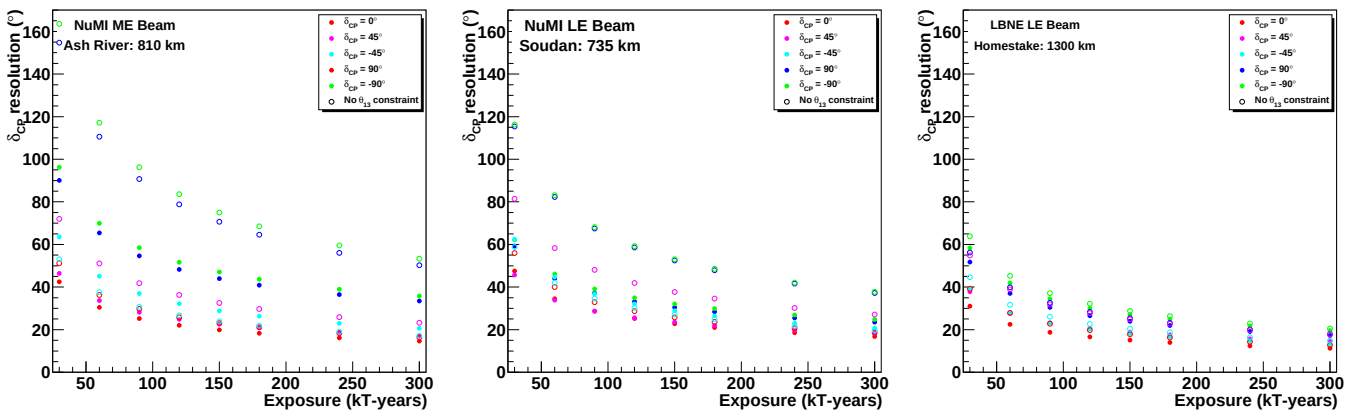

FIG. 11. The 1σ resolution on the measurement of δ_{cp} as a function of exposure in kt.yrs for $\delta_{cp} = 0$ (red), $\pi/4$ (magenta), $-\pi/4$ (cyan), $\pi/2$ (blue), $-\pi/2$ (green). The closed circles include the tight external constraint on θ_{13}. The open circles are without any external constraints on θ_{13}. The plots from left to right are for Ash River, Soudan, and LBNE-Homestake.

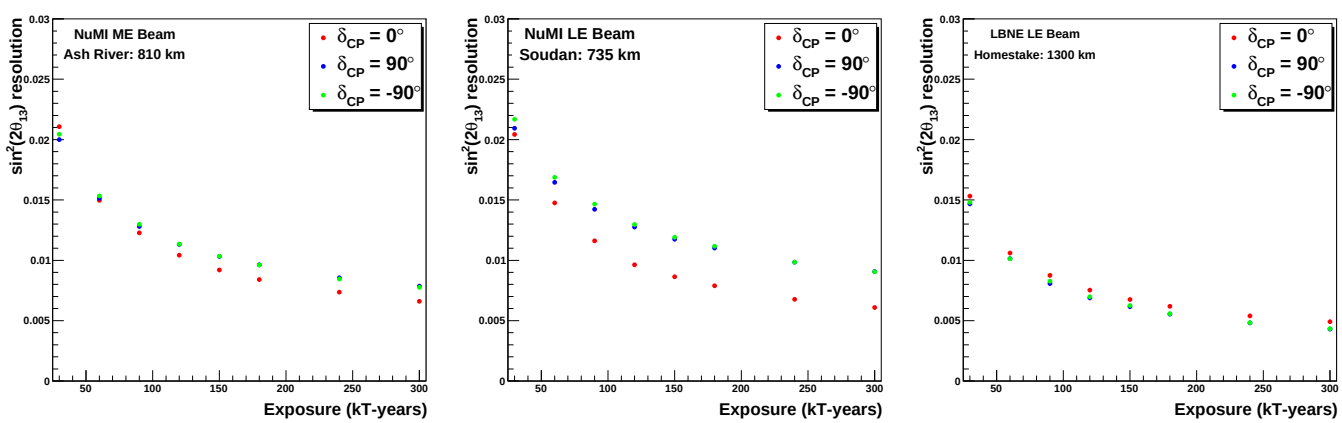

FIG. 12. The 1σ resolution on the measurement of $\sin^2 2\theta_{13}$ as a function of exposure in kt.yrs for $\delta_{cp} = 0$ (red), $\pi/2$ (blue), $-\pi/2$ (green). The plots from left to right are for Ash River, Soudan, and LBNE-Homestake.

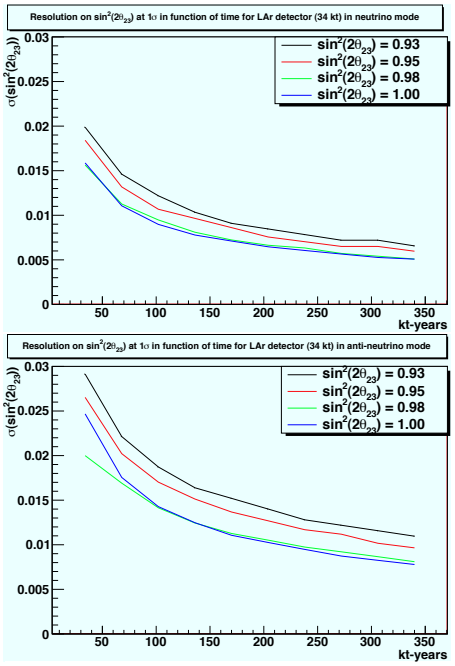

FIG. 13. The 1σ resolution on the measurement of $\sin^2 2\theta_{23}$ from $\nu_\mu \to \nu_\mu$ oscillations as a function of exposure in kt.yrs for different values of $\sin^2 2\theta_{23}$ for neutrinos (top) and anti-neutrinos (bottom). The plots from left to right are for Ash River, Soudan, and LBNE-Homestake.

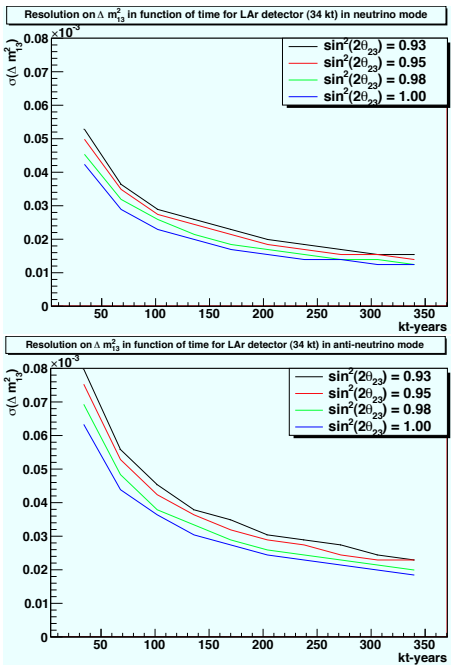

FIG. 14. The 1σ resolution on the measurement of Δm^2_{32} from $\nu_\mu \to \nu_\mu$ oscillations as a function of exposure in kt.yrs for different values of $\sin^2 2\theta_{23}$ for neutrinos (top) and anti-neutrinos (bottom). The plots from left to right are for Ash River, Soudan, and LBNE-Homestake.

D. Precision Measurement of Neutrino Mixing Parameters

E. Searches for New Physics

In addition to precision measurements of the standard three-flavor neutrino oscillation parameters, LBNE is also well-suited for new physics searches in the neutrino sector. For example, the experiment is sensitive to non-standard neutrino interactions and active-sterile neutrino mixing, provided that these effects are not too weak.

1. Non-standard Interactions

NC non-standard interactions (NSI) can be understood as non-standard matter effects that are visible only in a far detector at a sufficiently long baseline. This is where LBNE has a unique advantage compared to other long-baseline experiments (except atmospheric neutrino experiments, which are, however, limited by systematic effects). NC NSI can be parameterized as new contributions to the MSW matrix in the neutrino-propagation Hamiltonian:

$$H = U \begin{pmatrix} 0 & & \\ & \Delta m^2_{21}/2E & \\ & & \Delta m^2_{31}/2E \end{pmatrix} U^\dagger + \tilde{V}_{\rm MSW}\,, \tag{5}$$

with

$$\tilde{V}_{\rm MSW} = \sqrt{2} G_F N_e \begin{pmatrix} 1+\epsilon^m_{ee} & \epsilon^m_{e\mu} & \epsilon^m_{e\tau} \\ \epsilon^{m*}_{e\mu} & \epsilon^m_{\mu\mu} & \epsilon^m_{\mu\tau} \\ \epsilon^{m*}_{e\tau} & \epsilon^{m*}_{\mu\tau} & \epsilon^m_{\tau\tau} \end{pmatrix} \tag{6}$$

Here, U is the leptonic mixing matrix, and the ϵ-parameters give the magnitude of the NSI relative to standard weak interactions. For new physics scales of few $\times$ 100 GeV, we expect $|\epsilon| \lesssim 0.01$.

To assess the sensitivity of LBNE to NC NSI, the NSI discovery reach is defined in the following way: After simulating the expected event spectra, assuming given "true" values for the NSI parameters, one attempts a fit assuming no NSI. If the fit is incompatible with the simulated data at a given confidence level, one would say that the chosen "true" values of the NSI parameters are within the experimental discovery reach. Figure 15 shows the NSI discovery reach of LBNE for the case where only one of the $\epsilon^m_{\alpha\beta}$ parameters is non-negligible at a time [13].

It can be concluded from the figure that LBNE will be able to improve model-independent bounds on NSI in the e–μ sector by a factor of two, and in the e–τ sectors by an order of magnitude.

2. Long-Range Interactions

The small scale of neutrino-mass differences implies that minute differences in the interactions of neutrinos and antineutrinos with background sources can be detected through perturbations to the time evolution of the flavor eigenstates. The longer the experimental baseline, the higher the sensitivity to a new long-distance potential acting on neutrinos. For example, some of the models for such long-range interactions (LRI) as described in [14] could contain discrete symmetries that stabilize the proton and a dark matter particle and thus provide new connections between neutrino, proton decay and dark matter experiments. The longer baseline of LBNE coupled with the expected precision of better than 1% on the ν_μ and $\bar{\nu}_\mu$ oscillation parameters improves the sensitivity to LRI beyond that possible by the current generation of long-baseline neutrino experiments.

3. Search for Active-Sterile Neutrino Mixing

Searches for evidence of active sterile neutrino mixing at LBNE can be conducted by examining the NC event rate at the Far Detector and comparing it to a precision measurement of the expected rate from the near detector. Observed deficits in the NC rate could be evidence for active sterile neutrino mixing. The latest such search in a long baseline experiment was conducted by the MINOS experiment [Phys.Rev.D81:052004,2010]. The expected rate of NC interactions with visible energy > 0.5 GeV in LBNE is approximately 5K events over five years (see Table **??**). The NC identification efficiency is high with a low rate of ν_μ CC background misidentification as shown in Table V. LBNE will provide a unique opportunity to revisit this search with higher precision over a large range of neutrino energies.

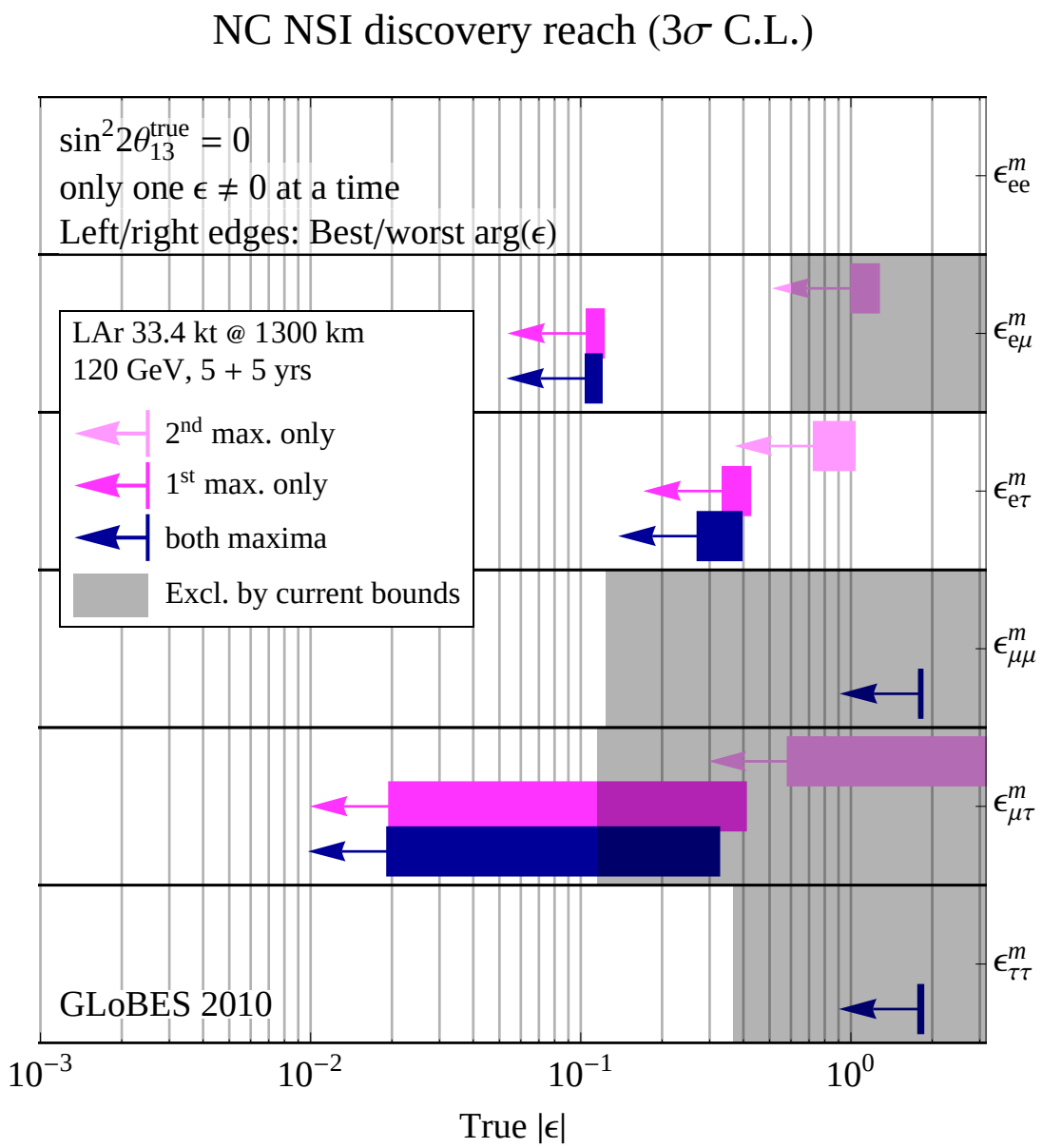

FIG. 15. Non-standard interaction discovery reach in a 34kT LAr-TPC at Homestake. The left and right edges of the error bars correspond to the most favorable and the most unfavorable values for the complex phase of the respective NSI parameters. Red arrows indicate the current model-independent limits on the different parameters at 3 σ [11? , 12].

F. Summary

Table VI summarizes the oscillation measurements achieved with different configurations.

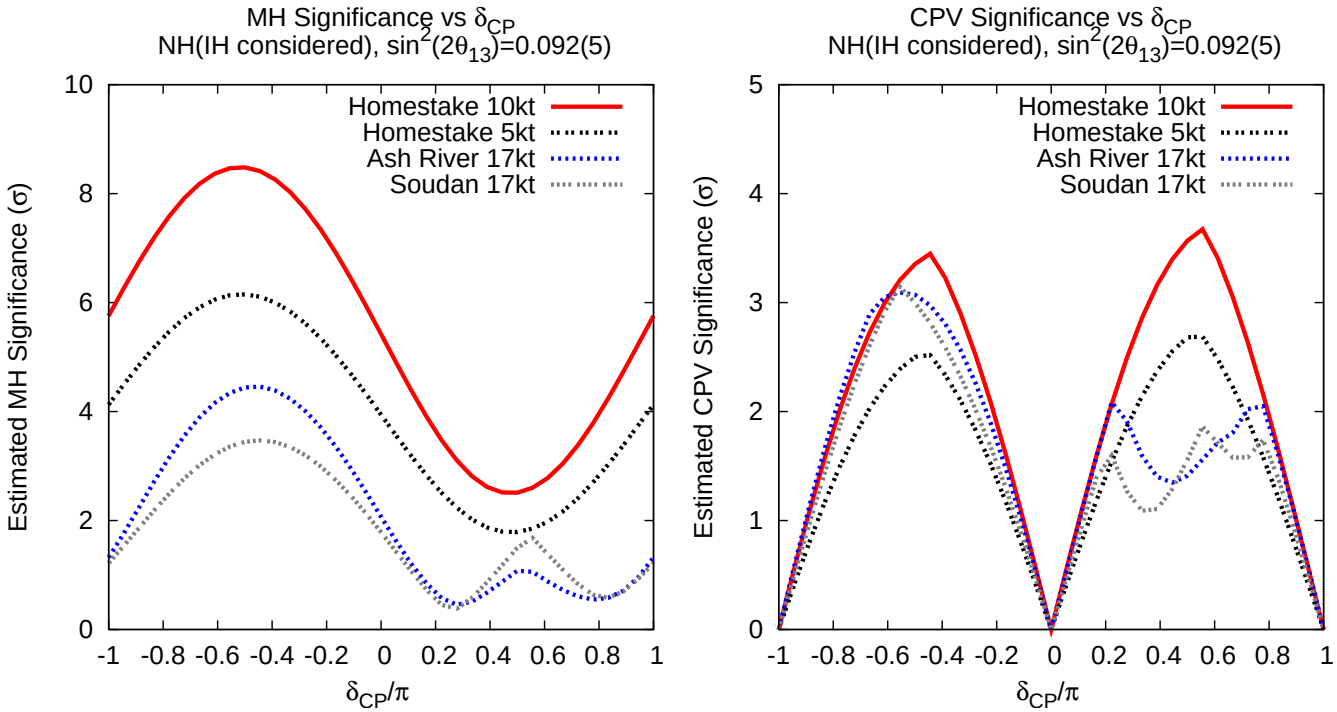

FIG. 16. The significance with which the mass ordering (left) and CP violation is resolved (right) for different configurations

TABLE VI. Summary of the oscillation measurements with different configurations

Configuration	MH fraction of δ (3σ)	CPV fraction of δ (3σ)	$\sigma(\delta_{cp})$ $0, 90^\circ$	$\sigma(\sin^2 2\theta_{13})$	$\sigma(\sin^2 2\theta_{23})$ ν	$\sigma(\Delta m^2_{32})$ ν (eV^2)	$\sigma(\sin^2 2\theta_{23})$ $\bar{\nu}$	$\sigma(\Delta m^2_{32})$ $\bar{\nu}$ (eV^2)
Soudan 10kt	0.5	0.09						
Soudan 15kt	0.52	0.26						
Soudan 34kt								
Soudan 10kt + NOνA/T2K	0.68	0.48						
Soudan 15kt + NOνA/T2K	0.74	0.53						
Soudan 34kt + NOνA/T2K								
Ash River 10kt	0.53	0						
Ash River 15kt	0.55	0						
Ash River 34kt								
Ash River 10kt + NOνA/T2K	0.8	0.5						
Ash River 15kt + NOνA/T2K	0.84	0.58						
Ash River 34kt + NOνA/T2K								
Homestake 5kt	0.7	0						
Homestake 10kt	0.9	0.25						
Homestake 15kt	1.0	0.50						
Homestake 34kt	1.0	0.70						

IV. NON-ACCELERATOR PHYSICS REACH

A large liquid argon TPC, when sited underground, has significant capability for addressing diverse physics topics: these capabilities are described in detail in reference [2]. For non-beam physics, no external trigger will be available, and therefore the key issue is selection of signal from background, assuming suitable triggering can be implemented. Photon collection will likely be required. Since backgrounds are dominated by cosmic rays, physics reach for a given detector size depends primarily on depth. Table VII summarizes expected signal rates. Proton decay and atmospheric neutrino events are, like beam events, ∼GeV scale, and should in principle be quite cleanly identifiable in a LArTPC. Proton decay events, although distinctive, would be extremely rare, and hence highly intolerant of background; in contrast, atmospheric neutrinos (which are background for proton decay) have a higher rate and could tolerate some background. The signatures of individual supernova burst neutrino interaction events are much less clean: with only a few tens of MeV of energy, these neutrinos will create small tracks involving only a few adjacent wires. For diffuse "relic" supernova events which arrive singly, the very low expected rate makes their selection overwhelmingly difficult, and we will not consider them here. A nearby core collapse is more promising: it will provide a pulse of low energy events all arriving within ∼30 seconds, so that we can hope to make a meaningful measurement of signal over a (well-known) background.

TABLE VII.

Physics	Energy range	Expected signal rate (events $\text{kton}^{-1}\text{s}^{-1}$)
Proton decay	$\sim$ GeV	$< 2 \times 10^{-9}$
Atmospheric neutrinos	$0.1 - 10$ GeV	$\sim 10^{-5}$
Supernova burst neutrinos	few-50 MeV	~ 3 in 30 s at 10 kpc
Diffuse supernova neutrinos*	20-50 MeV	$< 2 \times 10^{-9}$

We will consider the physics reach as a function of detector mass and depth for proton decay, supernova and atmospheric neutrinos.

Searches for baryon number non-conservation: Searches for baryon-number-violating processes are highly motivated by grand unified theories; even a single event could be evidence of physics beyond the Standard Model. Current limits are dominated by Super-K [**?**]; however for some predicted modes, most famously $p \to K^+\bar{\nu}$, efficiency for water Cherenkov detectors is low, and detectors which can cleanly reconstruct kaon decay products have a substantial efficiency advantage. Other modes for which LArTPCs have an edge include $n \to e^- K^+$ and $p \to e^+\gamma$. Figure 17 shows the expected limit as a function of time for $p \to K^+\bar{\nu}$. According to this plot, approximately 10 kton of LAr is required to improve the limits beyond continued Super-K running.

In LAr, the most pernicious background for proton decay with kaon final states comes from cosmic rays that produce kaons in photonuclear interactions in the rock near the detector. This type of background has been studied for LAr in references [**? ?**], with the conclusion that proton decay searches can be successful at moderate depth via reduction of fiducial mass or in conjunction with a high-quality veto, but cannot be done at the surface. Among the sites under consideration, Homestake would be excellent. Soudan would likely be acceptable, although would require some reduction in fiducial mass. Proton decay searches are not feasible for any of the surface options.

Atmospheric neutrinos: Atmospheric neutrinos are unique among sources used to study oscillations: the oscillated flux contains neutrinos and antineutrinos of all flavors, and matter effects play a significant role. Since the oscillation phenomenology plays out over several decades in energy and path length, atmospheric neutrinos are very sensitive to alternative explanations or subdominant new physics effects that predict something other than the characteristic (L/E) dependence predicted by oscillations in the presence of matter. The excellent CC/NC separation and the ability to fully reconstruct the hadronic final state in CC interactions in an LArTPC would enable the atmospheric neutrino 4-momentum to be fully reconstructed. This would enable a higher-resolution measurement of L/E to be extracted from atmospheric-neutrino events in an LArTPC compared to the measurements obtained from Super-K. The expected interaction rate is about 285 events per kton-year.

Since atmospheric neutrinos are somewhat more tolerant of background than proton decay, a depth which is sufficient for a proton decay search should also be fine for atmospheric neutrinos. For 4850 ft depth, a veto should not be necessary, and one can assume full fiducial mass; at Soudan depth, a 1 meter fiducial cut should be adequate. Figure 18 shows expected sensitivity to mass hierarchy: for ten years of running, a Soudan-depth 20 kton detector could rival beam sensitivity, and even a 10 kton detector would add to world knowledge.

Core-collapse supernova neutrinos: A nearby core-collapse supernova will provide a wealth of information via its neutrino signal (see [31, 32] for reviews). The neutrinos are emitted in a burst of a few tens of seconds duration.

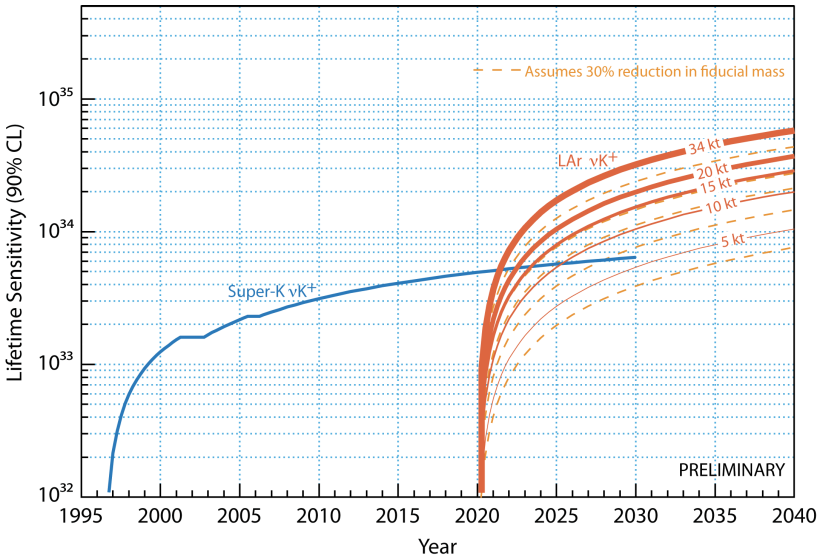

FIG. 17. Proton decay lifetime limit for $p \to K^+\bar{\nu}$ as a function of time for Super-Kamiokande compared to different LAr-FD masses at the 4850 level starting in 2020. The dashed lines show the effect of a 30% reduction of fiducial mass, conservatively assumed for a Soudan-depth detector. The limits are at 90% C.L., calculated for a Poisson process including background assuming that the detected events equal the expected background. (Figure from J. Raaf.)

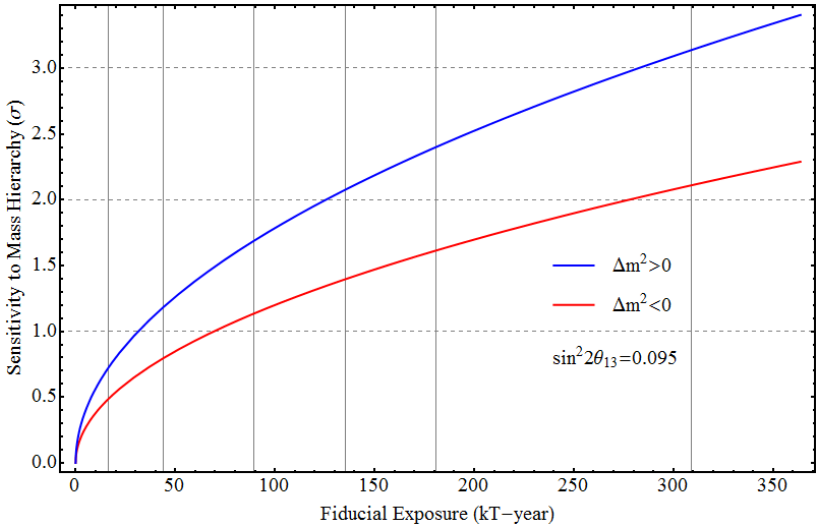

FIG. 18. Sensitivity to mass hierarchy using atmospheric neutrinos as a function of fiducial exposure in a LAr detector. (Figure from H. Gallagher, J. Coelho, A. Blake.)

Energies are in the few tens of MeV range, and luminosity is divided roughly equally between flavors. Ability to measure and tag the different flavor components of the spectrum is essential for extraction of physics and astrophysics from the signal. Currently, world-wide sensitivity is primarily to $\bar{\nu}_e$, via inverse beta decay on free protons, which dominates the interaction rate in water and liquid scintillator detectors. Liquid argon has a unique sensitivity to the *electron flavor* component of the flux, via the absorption interaction on ^{40}Ar, $\nu_e +^{40}\text{Ar} \to e^- +^{40}\text{K}^*$. In principle, this interaction can be tagged using the observed gamma cascade. About 3000 events would be expected in 34 kton of liquid argon at 10 kpc; the number of signal events scales with mass and inverse square of distance as shown in Fig. 19. For a collapse in the Andromeda galaxy, a 34-kton detector would expect about one event from Andromeda. This sensitivity would be lost for a smaller detector; however even a 5 kton detector would gather a unique ν_e signal from within the Milky Way.

As noted above, due to their low energy, supernova events are subject to background, although the burst nature of the signal means that the background can be well known and subtracted. Muons and their associated Michel electrons

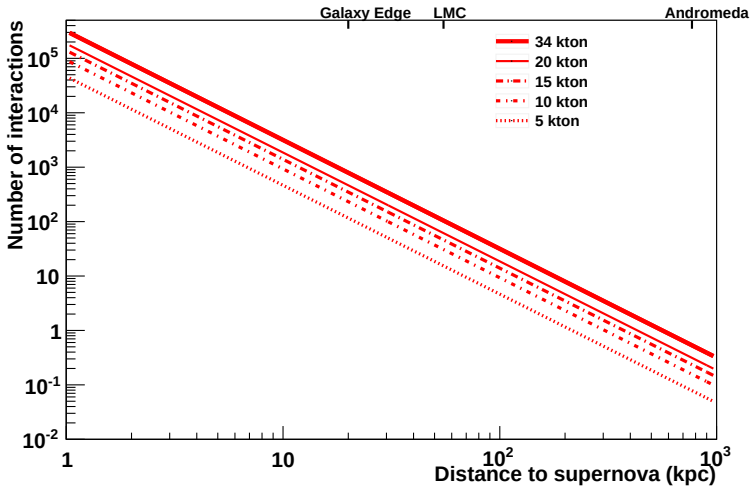

FIG. 19. Number of supernova neutrino interactions in a LAr detector as a function of distance to the supernova, for different detector masses. Most core collapses are expected to occur within 10-15 kpc, a few times per century.

can in principle be removed. Radioactivity, including cosmogenic spallation products, also tends to make <10 MeV signals, which lie below the main supernova signal range, but inhabit a potential region of interest for physics in the signal. Preliminary studies from reference [**?**] and extended for cosmic ray rates on the surface suggest that while Soudan depth is likely acceptable, the surface cosmic-ray associated signal rates are daunting, requiring at least a few orders of magnitude of background rejection to pull signal from background. While more work needs to be done to determine the extent to which the background can be mitigated, a surface option is highly unfavorable for supernova neutrino physics.

Summary: Although more work needs to be done to understand backgrounds at shallow depth, the following findings are fairly robust:

- Proton decay capabilities as a function of depth are the best documented, and a search at the surface seems impossible. A modest fiducial mass reduction would be required at Soudan. A detector of at least 10 kton would be needed for competitiveness.
- For atmospheric neutrinos, less is known about signal selection on the surface; however it is probably extremely difficult. Soudan depth is acceptable. Underground, a 20 kton detector would be needed for competitiveness, although a smaller detector could still provide useful information.
- For supernova burst neutrinos, selection of signal events over background at the surface will be a daunting task, and information will be highly degraded even in the best case. Soudan depth would be acceptable. More mass is better, but even a 5-kton detector would provide a unique ν_e-flavor supernova signal.

The overall conclusion: a reasonably-sized detector sited at 4850 ft depth would provide excellent opportunities for a diverse range of physics topics. Soudan depth requires only modest compromise in physics reach. At the surface, physics capabilities for non-beam topics are extremely poor.

V. SUMMARY

The summary.

[1] J.A. Formaggio and G.P. Zeller, "From eV to EeV: Neutrino Cross Sections Across Energy Scales", to be published in Rev. Mod. Phys. (2012)
[2] T. Akiri *et al.* [LBNE Collaboration] "The 2010 Interim Report of the Long-Baseline Neutrino Experiment Collaboration Physics Working Groups" arXiv:1110.6249
[3] "LBNE Liquid Argon TPC Detector Case Study" LBNE-doc-3600
[4] "A Proposal for a Detector 2 km Away from the T2K Neutrino Source", `http://www.phy.duke.edu/~cwalter/nusag-members/`.
[5] "A Large Liquid Argon Time Projection Chamber for Long-baseline Off-Axis Neutrino Oscillation Physics with the NuMI Beam", Submitted to the NuSAG committee, 2006, FERMILAB-FN-0776-E.
[6] P. Adamson *et al.* [MINOS Collaboration] "Improved search for muon-neutrino to electron-neutrino oscillations in MINOS" Phys.Rev.Lett.107:181802,2011, arXiv:1108.0015v11
[7] A. Ankowski *et al.* [ICARUS Collaboration], Acta Physica Polonica B **41**, 103 (2010).
[8] S. Amoruso *et al.* [ICARUS Collaboration], Eur. Phys. J. **C33**, 233 (2004).
[9] A. Ankowski *et al.* [ICARUS Collaboration], Eur. Phys. J. **C48**, 667 (2006).
[10] P. Adamson *et al.* [MINOS Collaboration] "Search for the disappearance of muon antineutrinos in the NuMI neutrino beam." FERMILAB-PUB-11-357-PPD, BNL-96122-2011-JA, Phys.Rev.D84:071103,2011. arXiv:1108.1509
[11] S. Davidson, C. Pena-Garay, N. Rius, and A. Santamaria, hep-ph/0302093.
[12] M.C. Gonzalez-Garcia, and M. Maltoni, Phys. Rept. **460**, 1 (2008), arXiv:0704.1800 [hep-ph].
[13] arXiv:1010.3706 and private communication with Joachim Kopp.
[14] H. Davoudiasl, H.S. Lee and W. J. Marciano, Phys. Rev. D 84 031009 (2011) arXiv:1102.5352[hep.ph]
[15] The LArSoft Collaboration, `https://plone4.fnal.gov:4430/P1/Main/wiki/LArSoft/LArSoft`
[16] J. C. Pati and A. Salam, Phys. Rev. Lett. **31**, 661 (1973).
[17] H. Georgi and S. L. Glashow, Phys. Rev. Lett. **32**, 438 (1974).
[18] S. Dimopoulos, S. Raby and F. Wilczek, Phys. Lett. B **112**, 133 (1982).
[19] P. Langacker, Phys. Rept. **72**, 185 (1981).
[20] W. de Boer, Prog. Part. Nucl. Phys. **33**, 201 (1994) [arXiv:hep-ph/9402266].
[21] P. Nath and P. Fileviez Perez, Phys. Rept. **441**, 191 (2007) [arXiv:hep-ph/0601023].
[22] S. Raby *et al.*, arXiv:0810.4551 [hep-ph].
[23] G. Senjanovic, AIP Conf. Proc. **1200**, 131 (2010) [arXiv:0912.5375 [hep-ph]].
[24] T. Li, D. V. Nanopoulos and J. W. Walker, arXiv:1003.2570 [hep-ph].
[25] A. Bueno *et al.*, JHEP **0704**, 041 (2007) [arXiv:hep-ph/0701101].
[26] R. M. Barnett *et al.* [Particle Data Group], Phys. Rev. D **54**, 1 (1996).
[27] H. Nishino *et al.* [Super-Kamiokande Collaboration], Phys. Rev. Lett. **102**, 141801 (2009) [arXiv:0903.0676 [hep-ex]].
[28] `http://www-sk.icrr.u-tokyo.ac.jp/whatsnew/new-20091125-e.html`
[29] Y. Hayato *et al.* [Super-Kamiokande Collaboration], Phys. Rev. Lett. **83**, 1529 (1999) [arXiv:hep-ex/9904020].
[30] K. Kobayashi *et al.* [Super-Kamiokande Collaboration], Phys. Rev. D **72**, 052007 (2005) [arXiv:hep-ex/0502026].
[31] K. Scholberg, arXiv:astro-ph/0701081.
[32] A. Dighe, arXiv:0809.2977 [hep-ph].
[33] R. M. Bionta *et al.*, Phys. Rev. Lett. **58**, 1494 (1987).
[34] K. Hirata *et al.* [KAMIOKANDE-II Collaboration], Phys. Rev. Lett. **58**, 1490 (1987).
[35] A. Mirizzi, G. G. Raffelt and P. D. Serpico, JCAP **0605**, 012 (2006) [arXiv:astro-ph/0604300].
[36] S. Choubey, B. Dasgupta, A. Dighe and A. Mirizzi, arXiv:1008.0308 [hep-ph].
[37] G. G. Raffelt, arXiv:astro-ph/9707268.
[38] S. Hannestad and G. Raffelt, Phys. Rev. Lett. **87**, 051301 (2001) [arXiv:hep-ph/0103201].
[39] P. Antonioli *et al.*, New J. Phys. **6**, 114 (2004) [arXiv:astro-ph/0406214].
[40] K. Scholberg, Astron. Nachr. **329**, 337 (2008) [arXiv:0803.0531 [astro-ph]].
[41] K. Scholberg, J. Phys. Conf. Ser. **203**, 012079 (2010).
[42] `http://www.mpi-hd.mpg.de/lin/globes/`
[43] T. Totani, K. Sato, H. E. Dalhed and J. R. Wilson, Astrophys. J. **496**, 216 (1998) [arXiv:astro-ph/9710203].
[44] J. Gava, J. Kneller, C. Volpe and G. C. McLaughlin, Phys. Rev. Lett. **103**, 071101 (2009) [arXiv:0902.0317 [hep-ph]].
[45] H. Duan and A. Friedland, arXiv:1006.2359 [hep-ph].
[46] M. T. Keil, G. G. Raffelt and H. T. Janka, Astrophys. J. **590**, 971 (2003) [arXiv:astro-ph/0208035].
[47] E. Kolbe, K. Langanke and P. Vogel, Phys. Rev. D **66**, 013007 (2002).
[48] K. Langanke, P. Vogel and E. Kolbe, Phys. Rev. Lett. **76**, 2629 (1996) [arXiv:nucl-th/9511032].
[49] J. F. Beacom and P. Vogel, Phys. Rev. D **60**, 033007 (1999) [arXiv:astro-ph/9811350].
[50] R. Tomas, D. Semikoz, G. G. Raffelt, M. Kachelriess and A. S. Dighe, Phys. Rev. D **68**, 093013 (2003) [arXiv:hep-ph/0307050].
[51] M. Ikeda, `http://www-sk.icrr.u-tokyo.ac.jp/sk/pub/m\_ikeda\_mron.pdf`
[52] M. Ikeda *et al.* [Super-Kamiokande Collaboration], Astrophys. J. **669**, 519 (2007) [arXiv:0706.2283 [astro-ph]].
[53] I. Gil Botella and A. Rubbia, JCAP **0408**, 001 (2004) [arXiv:hep-ph/0404151].
[54] E. Kolbe, K. Langanke, G. Martinez-Pinedo and P. Vogel, J. Phys. G **29**, 2569 (2003) [arXiv:nucl-th/0311022].

[55] T. Totani, K. Sato and Y. Yoshii, Astrophys. J. **460**, 303 (1996) [arXiv:astro-ph/9509130].
[56] K. Sato, T. Totani and Y. Yoshii, *Prepared for 4th SFB-375 Ringberg Workshop on Neutrino Astrophysics, Ringberg Castle, Tegernsee, Germany, 20-24 Oct 1997*
[57] D. H. Hartmann and S. E. Woosley, Astropart. Phys. **7**, 137 (1997).
[58] R. A. Malaney, Astropart. Phys. **7**, 125 (1997) [arXiv:astro-ph/9612012].
[59] M. Kaplinghat, G. Steigman and T. P. Walker, Phys. Rev. D **62**, 043001 (2000) [arXiv:astro-ph/9912391].
[60] S. Ando, J. F. Beacom and H. Yuksel, Phys. Rev. Lett. **95**, 171101 (2005) [arXiv:astro-ph/0503321].
[61] C. Lunardini, Phys. Rev. D **75**, 073022 (2007) [arXiv:astro-ph/0612701].
[62] M. Fukugita and M. Kawasaki, Mon. Not. Roy. Astron. Soc. **340**, L7 (2003) [arXiv:astro-ph/0204376].
[63] A. Lien, B. D. Fields and J. F. Beacom, Phys. Rev. D **81**, 083001 (2010) [arXiv:1001.3678 [astro-ph.CO]].
[64] J. F. Beacom, arXiv:1004.3311 [astro-ph.HE].
[65] C. Lunardini, arXiv:1007.3252 [astro-ph.CO].
[66] M. Malek *et al.* [Super-Kamiokande Collaboration], Phys. Rev. Lett. **90**, 061101 (2003) [arXiv:hep-ex/0209028].
[67] L. E. Strigari, M. Kaplinghat, G. Steigman and T. P. Walker, JCAP **0403**, 007 (2004) [arXiv:astro-ph/0312346].
[68] J. F. Beacom and M. R. Vagins, Phys. Rev. Lett. **93**, 171101 (2004) [arXiv:hep-ph/0309300].
[69] H. Watanabe *et al.* [Super-Kamiokande Collaboration], arXiv:0811.0735 [hep-ex].
[70] A. Kibayashi and S. K. Collaboration, arXiv:0909.5528 [astro-ph.IM].
[71] Y. Koshio, Ph.D thesis, University of Tokyo (1998)
[72] `http://www.phys.hawaii.edu/~jgl/post/A~White~Paper~for~Large~Liquid~Scintillation~Detectors~at~DUSEL.pdf`
[73] P. Vogel and J. F. Beacom, Phys. Rev. D **60**, 053003 (1999) [arXiv:hep-ph/9903554].
[74] A. Strumia and F. Vissani, Phys. Lett. B **564**, 42 (2003) [arXiv:astro-ph/0302055].
[75] W. E. Ormand, P. M. Pizzochero, P. F. Bortignon and R. A. Broglia, Phys. Lett. B **345**, 343 (1995) [arXiv:nucl-th/9405007].
[76] M. Sajjad Athar and S. K. Singh, Phys. Lett. B **591**, 69 (2004).
[77] A. G. Cocco, A. Ereditato, G. Fiorillo, G. Mangano and V. Pettorino, JCAP **0412**, 002 (2004) [arXiv:hep-ph/0408031].
[78] `http://nucleardata.nuclear.lu.se/nucleardata/toi/nuclide.asp?iZA=30011`
[79] A. Rubbia, J. Phys. Conf. Ser. **171**, 012020 (2009) [arXiv:0908.1286 [hep-ph]].
[80] O.L.G. Peres *et al.*, Phys. Rev. **D79**, 113002 (2009).
[81] J. Bernabeu *et al.*, Nucl. Phys. **B669**, 255 (2003).
[82] M.C. Gonzalez-Garcia *et al.*, Phys. Rev. **D70**, 093005 (2004).
[83] O.L.G. Peres *et al.*, Phys. Lett. **B456**, 204 (1999).
[84] Akhmedov *et al.*, JHEP 0806 072 (2008).
[85] S.T. Petcov *et al.*, Nucl. Phys. **B**, 740 (2006).
[86] S. Palomares-Ruiz *et al.*, Nucl. Phys. **B712**, 392 (2005).
[87] Y. Ashie *et al.*, Phys. Rev. Lett **93**, 101801 (2004).
[88] Y. Ashie *et al.*, Phys.Rev. **D71**, 112005 (2005).
[89] K. Abe *et al.*, Phys. Rev. Lett. **97**, 171801 (2006).
[90] R. Wendell *et al.*, arXiv:1002.3471 (hep-ex) (2010).
[91] J. Hosaka *et al.*, Phys. Rev. **D74**, 032002 (2006).
[92] K. Abe *et al.*, Phys. Rev. **D77**, 052001 (2008).
[93] W. Wang, Ph. D Thesis (2007).
[94] G. Mitsuka Ph. D Thesis (2009).
[95] P. Adamson *et al.*, Phys. Rev. **D75**, 092003 (2007).
[96] D. Indumathi *et al.*, Phys. Rev. **D71**, 013001 (2005).
[97] S. Coleman and S. Glashow, Phys. Lett. **B405**, 249 (1997).
[98] F. Klinkhamer and G. Volovik, Intl. Jour. of Mod. Phys. **A20**, 2795 (2005).
[99] D. Colladay and V. Kostelecky, Phys. Rev. **D**, 116002 (1998).
[100] Y. Grossman *et al.*, Phys. Rev. **D72**, 125001 (2005).
[101] M. C. Gonzalez-Garcia *et al.*, Nucl. Phys. **B573**, 3 (2000).
[102] D. Kaplan *et al.*, Phys. Rev. Lett. **93**, 091801 (2004).
[103] J. Conrad *et al.*, arXiv:1008.2984/hep-ph (2010).
[104] P. Huber *et al.*, arXiv:0501037/hep-ph (2005).
[105] A. Rubbia, NNN99 Proceedings, arXiv:0001052/hep-ex (2001).
[106] M. Fechner *et al.*, Phys. Rev. **D79**, 112010 (2009).
[107] S. Petcov and T. Schwetz, arXiv:0511277/hep-ph (2005).
[108] C. Andreopoulos *et al.*, Nucl. Instrum. Meth. **A614**, 87 (2010).
[109] G. Barr *et al.*, Phys. Rev. **D70**, 023006 (2004).
[110] G. Battistoni *et al.*, Astropart. Phys. **19**, 269 (2003).
[111] T. Kajita, Talk at NOON2004 (Tokyo), 2004.
[112] M. Ishitsuka, Ph. D Thesis (2004).
[113] A. Bueno *et al.*, arXiv:0701101/hep-ph (2007).
[114] R. Gandhi *et al.*, Phys. Rev. D78:073001 (2008).
[115] F. Dufour, Ph. D Thesis (2009).

[116] V. Barger *et al.*, Phys. Rev. **D22**, 2718 (1980).
[117] M. Messier, private communication (2010).
[118] M. Sanchez *et al.*, Phys. Rev. **D68**, 113004 (2003).
[119] C. Ishihara, Ph. D Thesis (2010).
[120] J.G. Learned and K. Mannheim, Ann. Rev. Nucl. Part. Sci. **50** 679 (2000)
[121] Bahcall, J., Waxmann, E., 2001, Physical Review D, **64** 023002 (2001)
[122] Gueta, *et al.*, Astropart.Phys. **20** 429-455 (2004)
[123] M. Drees and M. M. Nojiri, Phys. Rev. D **47**, 376 (1993)
[124] DeYoung, T., *et al.*et al. (IceCube Collaboration), 2008. J. of Phys. Conf. Ser. **136** 022046 (2008)
[125] V. Aynutdinov,*et al.* (BAIKAL Collaboration), Astropart.Phys.25:140-150,2006
[126] The Antares Collaboration Internal Report CPPM-P-1999-02 (1999), arXiv:astro-ph/9907432v1
[127] IceCube collaboration, in preparation.
[128] R. Abbasi, *et al.*, Astrophys.J **701** L47-L51 (2009)
[129] M. Ackermann, *et al.*, Astrophys.J **675** 1014 (2008)
[130] R. Abbasi, *et al.*, Astrophys.J. **710** 346-359 (2010)
[131] R. Abbasi, *et al.*, Phys. Rev. Lett. **102** 201302 (2009), arXiv:0910.4480
[132] S. Desai, *et al.*, Phys.Rev.D **70** 083523 (2004)
[133] E. Thrane, *et al.*, Astrophys.J **704** 503-512 (2009)
[134] M.E.C Swanson, *et al.*, Astrophys.J **652** 206-215 (2006)
[135] Private collaboration document DUSEL/LBNE R&D Document 994, `http://nwg.phy.bnl.gov/DDRD/cgi-bin/private/ShowDocument?docid=994`
[136] E. Presani, *et al.*, Nuclear Physics B Proceedings Supplements **188** 270-272 (2009)
[137] H. Yuksel, S. Horiuchi, J. Beacom, S. Ando, Phys.Rev.D **76** 123506 (2007)
[138] B. T. Cleveland et al. **Astrophys. J. 496: 505** (1998).
[139] S. Fukuda et al., Phys. Rev. Lett. **86**, 5651 (2001); Q. R. Ahmad et al., Phys. Rev. Lett. **87), 071301**(2001).
[140] Phys.Rev. **D69**, 011104 (2004).
[141] A. Guglielmi, talk at XXIV Neutrino Conference (Neutrino 2010), Athens, Greece (June 2010).
[142] Internal collaboration document DUSEL/LBNE R&D Document 643-v2, "Reference Near Detector Parameters," `http://nwg.phy.bnl.gov/DDRD/html/0006/000643/002/Near%20Detector%20Reference%20Parameters.docx`
[143] G.P. Zeller, "Expected Event Rates in the LBNE Near Detectors", docdb #783, `http://nwg.phy.bnl.gov/DDRD/html/0007/000783/001/event-rates.pdf`, flux files in `http://www.phy.bnl.gov/~bishai/nwg/work/gnumi/prod/`
[144] D. Casper, Nucl. Phys. Proc. Suppl. **112**, 161 (2002), hep-ph/0208030.
[145] R. Petti and G.P. Zeller, "Nuclear Effects in Water vs. Argon", docdb #740.
[146] G.P. Zeller et al., Phys. Rev. Lett. **88**, 091802 (2002); erratum-ibid. **90**, 239902 (2003)
[147] W.J. Marciano and Z. Parsa, J. Phys. G **29** (2003) 2629-2645.
[148] I. Stancu et al., arXiv:0910.2698 [hep-ex]
[149] The OscSNS Neutrino Experiment `http://physics.calumet.purdue.edu/~oscsns/`
[150] B. Baibussinov et al., arXiv:0909.0355 [hep-ex]
[151] J.A. Harvey, C.T. Hill and R.J. Hill, Phys. Rev. Lett. **99** (2007) 261601; Phys. Rev. D **77** (2008) 085017
[152] J. Jenkins and T. Goldman, Phys. Rev. D **80** (2009) 053005
[153] M.Shiozawa, Talk at NNN09; `http://nnn09.colostate.edu/Talks/Session02/091007-Shiozawa-Nucleon-decay-searches-dist.pdf`
[154] S.Mine *et al.* (K2K Collaboration), Phys. Rev. D 77, 032003 (2008); H. Nishino *et al.* (Super-Kamiokande Collaboration), Phys. Rev. Lett. 102, 141801 (2009).
[155] P. Astier et al. [NOMAD collaboration], Nucl. Phys. B621/1-2 (2001) 3-34, hep-ex/0111057
[156] D. Naumov et al. [NOMAD collaboration], Nucl.Phys.B 700 (2004) 51-68, hep-ex/0409037
[157] S. Alekhin, S. A. Kulagin, and R. Petti, AIP Conf. Proc. **967**, 215 (2007).
[158] S. Alekhin, S. Kulagin, and R. Petti, (2008), arXiv:0810.4893 [hep-ph].
[159] S. Alekhin, S. Kulagin and R. Petti, Phys. Lett. B **675**, 433 (2009).
[160] A. B. Arbuzov, D. Y. Bardin and L. V. Kalinovskaya, JHEP **78**, 506 (2005); arXiv:hep-ph/0407203.
[161] S. A. Kulagin and R. Petti, Nucl. Phys. **A765**, 126 (2006).
[162] S. A. Kulagin and R. Petti, Phys. Rev. **D76**, 094023 (2007).
[163] S. A. Kulagin and R. Petti, arXiv:1004.3062 [hep-ph].
[164] R. Petti and O. Samoylov, Proceedings of DIS10 - Firenze, Italy, 19-23 April 2010.
[165] A. Czarnecki and W.J. Marciano, Int. J. Mod. Phy. A15 (2000) 2365
[166] S.C. Bennet and C.E. Wieman, Phys. Rev. Lett. 82 (1999) 2484
[167] Particle Data Group, W.-M. Yao et al., Journal of Physics, G 33 (2006) 1
[168] P.L. Anthony et al [E158 collaboration], Phys.Rev.Lett. 95 (2005) 081601, hep-ex/0504049
[169] R. D. Young, J. Roche, R. D. Carlini and A. W. Thomas, Phys. Rev. Lett. **97**, 102002 (2006).
[170] D. B. Leinweber *et al.*, Phys. Rev. Lett. **94**, 212001 (2005).
[171] A. Airapetian *et al.*, Phys. Lett. B **666**, 446 (2008).
[172] L.A. Ahrens et al., Phys. Rev. D **35**, 785 (1987)
[173] G. Garvey et al., Phys. Rev. C **48**, 761 (1993)
[174] W.M. Alberico et al., Nucl. Phys. A **651**, 277 (1999)

[175] L. Bugel et al., arXiv:hep-ex/0402007
[176] A. Boyarsky, O. Ruchayskiy and M. Shaposhnikov, Ann. Rev. Nucl. Part. Sci. **59** (2009) 191 [arXiv:0901.0011 [hep-ph]]
[177] M. Shaposhnikov, JHEP **0808** (2008) 008 [arXiv:0804.4542 [hep-ph]].
[178] L. Canetti and M. Shaposhnikov, arXiv:1006.0133 [hep-ph].
[179] A. M. Cooper-Sarkar *et al.* [WA66 Collaboration], Phys. Lett. B **160** (1985) 207.
[180] F. Bergsma *et al.* [CHARM Collaboration], Phys. Lett. B **166** (1986) 473.
[181] A. Vaitaitis *et al.* [NuTeV Collaboration], Phys. Rev. Lett. **83** (1999) 4943 [arXiv:hep-ex/9908011].
[182] G. Bernardi *et al.*, Phys. Lett. B **166** (1986) 479.
[183] G. Bernardi *et al.*, Phys. Lett. B **203** (1988) 332.
[184] A. Atre, T. Han, S. Pascoli and B. Zhang, JHEP **0905** (2009) 030 [arXiv:0901.3589 [hep-ph]].
[185] D. Gorbunov and M. Shaposhnikov, JHEP **0710** (2007) 015 [arXiv:0705.1729 [hep-ph]].
[186] M. Soderberg, arXiv:0910.3433 [physics.ins-det]
[187] M. Maltoni and T. Schwetz, arXiv:0705.0107 [hep-ph]
[188] B. L. Ioffe, V. A. Khoze and L. N. Lipatov, "Hard Processes. Vol. 1: Phenomenology, Quark Parton Model," *Amsterdam, Netherlands: North-holland (1984) 340p*
[189] D. Allasia et al., Z. Physik C **28** (1985) 321-333.
[190] A. Accardi, M. E. Christy, C. E. Keppel, P. Monaghan, W. Melnitchouk, J. G. Morfin and J. F. Owens, Phys. Rev. D **81**, 034016 (2010).
[191] Jefferson Lab experimental proposal PR12-06-13, S. Bültmann, M. E. Christy, H. Fenker, K. A. Griffioen, C. E. Keppel, S. E. Kuhn, W. Melnitchouk and V. Tsvaskis, spokespersons, `http://www.jlab.org/exp$\_$prog/proposals/06/PR12-06-113.pdf`.
[192] A. Bodek and A. Simon, Z. Phys. C **29**, 231 (1985); G. T. Jones *et al.*, Z. Phys. C **44**, 379 (1989).
[193] M. Messier, UMI-99-23965; E.A. Paschos and J.Y. Yu, Phys. Rev. **D65**, 033002 (2002).
[194] Internal collaboration presentsation DUSEL/LBNE R&D Document 972, "Efficiencies for LAr20 for GLOBES," B. Fleming, Long-Baseline TG meeting (7/26/2010), `http://nwg.phy.bnl.gov/DDRD/cgi-bin/private/ShowDocument?docid=972`
[195] C. Yanagisawa, C.K. Jung, and P.T. Lee, `http://ale.physics.sunysb.edu/uno/publications/numunuePREBWv3.pdf`
[196] M. Diwan, private communication.
[197] B. Fleming, private communication and discussion at INT, August 2010.
[198] J. Kopp, docdb #770.
[199] J. Hosaka *et al.* [Super-Kamiokande Collaboration], Phys. Rev. D **73**, 112001 (2006) [arXiv:hep-ex/0508053].
[200] J. P. Cravens *et al.* [Super-Kamiokande Collaboration], Phys. Rev. D **78**, 032002 (2008) [arXiv:0803.4312 [hep-ex]].
[201] S. Amoruso *et al.* [ICARUS Collaboration], Eur. Phys. J. C **33**, 233 (2004) [arXiv:hep-ex/0311040].